Available online at www.sciencedirect.com

ScienceDirect

www.elsevier.com/locate/brainres

Research Report

Comparative evaluation of transport mechanisms of *trans*-1-amino-3-[^{18}F]fluorocyclobutanecarboxylic acid and L-[methyl-^{11}C]methionine in human glioma cell lines

Masahiro Ono[a,b], *Shuntaro Oka*[a,*], *Hiroyuki Okudaira*[a], *David M. Schuster*[c], *Mark M. Goodman*[c], *Keiichi Kawai*[b], *Yoshifumi Shirakami*[a]

[a]*Research Center, Nihon Medi-Physics Co., Ltd., Chiba 299-0266, Japan*
[b]*Division of Health Sciences, Graduate School of Medical Science, Kanazawa University, Ishikawa 920-0942, Japan*
[c]*Division of Nuclear Medicine and Molecular Imaging, Department of Radiology and Imaging Science, Emory University, Atlanta, GA 30322, USA*

ARTICLE INFO

Article history:
Accepted 21 August 2013
Available online 27 August 2013

Keywords:
anti-FACBC
Methionine
Glioma
Amino acid transporter
ASCT2
LAT1

ABSTRACT

Positron emission tomography (PET) with amino acid tracers is useful for the visualization and assessment of therapeutic effects on gliomas. Our purpose is to elucidate the transport mechanisms of *trans*-1-amino-3-[^{18}F]fluorocyclobutanecarboxylic acid (*anti*-[^{18}F]FACBC) and L-[methyl-^{11}C]methionine ([^{11}C]Met) in normal human astrocytes (NHA), low-grade (Hs683, SW1088), and high-grade (U87MG, T98G) human glioma cell lines. Because the short half-lives of fluorine-18 and carbon-11 are inconvenient for *in vitro* experiments, *trans*-1-amino-3-fluoro[1-^{14}C]cyclobutanecarboxylic acid (*anti*-[^{14}C]FACBC) and L-[methyl-^{14}C]methionine ([^{14}C]Met) were used instead of the PET tracers. Time-course uptake experiments showed that uptake of *anti*-[^{14}C]FACBC was 1.4–2.6 times higher than that of [^{14}C]Met in NHA and low-grade glioma cells, and was almost equal to that of [^{14}C]Met in high-grade glioma cells. To identify the amino acid transporters (AATs) involved in the transport of *anti*-[^{14}C]FACBC and [^{14}C]Met, we carried out competitive inhibition experiments using synthetic/naturally-occurring amino acids as inhibitors. We found that *anti*-[^{14}C]FACBC uptake in the presence of Na^+ was strongly inhibited by L-glutamine and L-serine (the substrates for ASC system AATs), whereas L-phenylalanine and 2-amino-bicyclo[2,2,1]heptane-2-carboxylic acid (BCH, the substrates for L system AATs) robustly inhibited Na^+-independent *anti*-[^{14}C]FACBC uptake. Regardless of Na^+, [^{14}C]Met uptake was inhibited strongly by L-phenylalanine and BCH. Moreover, the exchange transport activity of L-glutamine for *anti*-[^{14}C]FACBC was stronger than that of BCH in the presence of Na^+, whereas that for [^{14}C]Met was almost equal to BCH. These results demonstrate that ASC

Abbreviations: AAT(s), amino acid transporter(s); *anti*-[^{14}C]FACBC, *trans*-1-amino-3-fluoro[1-^{14}C]cyclobutanecarboxylic acid; *anti*-[^{18}F]FACBC, *trans*-1-amino-3-[^{18}F]fluorocyclobutanecarboxylic acid; BCH, 2-amino-bicyclo[2,2,1]heptane-2-carboxylic acid; [^{11}C]Met, L-[methyl-^{11}C]methionine; [^{14}C]Met, L-[methyl-^{14}C]methionine; MeAIB, 2-(methylamino)-isobutyric acid; NEM, N-ethylmaleimide; PET, positron emission tomography

*Corresponding author. Fax: +81 438 62 6969.
E-mail address: shuntaro_oka@nmp.co.jp (S. Oka).

0006-8993/$ - see front matter © 2013 Elsevier B.V. All rights reserved.
http://dx.doi.org/10.1016/j.brainres.2013.08.037

and L are important transport systems for *anti*-[^{18}F]FACBC uptake, while system L is predominantly involved in [^{11}C]Met transport in human astrocytes and glioma cells.

© 2013 Elsevier B.V. All rights reserved.

1. Introduction

With their invasive and proliferative potential, gliomas are fatal lesions that are the most frequent primary brain tumors in adult humans (Swanson et al., 2002). The current standard of clinical treatment comprises surgical resection followed by radiation therapy and chemotherapy. Although improvements in surgery, radiotherapy, and chemotherapy are associated with an improved prognosis (Clarke et al., 2010; Gorlia et al., 2008), a recent study reported that the 2-year survival rate of grade III patients is 65%, and that of grade IV is 31% (Cho et al., 2010). In particular, infiltrative and diffuse tumor that cannot be completely surgically excised are believed to be responsible for glioma treatment failure (Nazzaro and Neuwelt, 1990; Swanson et al., 2002). Therefore, precise identification of tumor size and extent is required for effective cancer therapy.

Positron emission tomography (PET) is useful for the detection and delineation of gliomas, and L-[methyl-^{11}C]methionine ([^{11}C]Met) is well studied as a PET tracer (Kracht et al., 2004). However, because of the short half-life of ^{11}C (20 min), the use of ^{11}C-labeled PET tracers is restricted to those facilities with an on-site cyclotron. To overcome these problems, ^{18}F (half-life: 110 min)-labeled amino acid analogs such as *trans*-1-amino-3-[^{18}F]fluorocyclobutanecarboxylic acid (*anti*-[^{18}F]FACBC) were developed (Shoup et al., 1999), and the feasibility of *anti*-[^{18}F]FACBC and [^{11}C]Met for imaging human gliomas has been reported (Akhurst et al., 2006).

Anti-[^{18}F]FACBC is a synthetic amino acid and is therefore believed to be transported into cells by amino acid transporters (AATs) (Oka et al., 2012; Okudaira et al., 2011). To date, more than 40 types of AATs have been identified. They are divided into two groups by whether the driving force for transport needs Na^+, and some Na^+-dependent AATs (*e.g.* the N and y^+L systems) can maintain transport activity when Li^+ is substituted for Na^+ (Fei et al., 2000; Kanai et al., 2000; Nakanishi et al., 2001a, 2001b). Moreover, it is known that AAT activities are affected by extracellular pH. For example, system L activities increase in low pH conditions, but system N activities decrease (Fei et al., 2000; Nakanishi et al., 2001a, 2001b). In terms of transport types, ASC, y^+L, asc, $b^{0,+}$, X_G^- and L AAT systems are exchangers that exchange their extracellular and intracellular substrates with a 1:1 stoichiometry (SLC tables, 2013, see "*References*"). Among these AATs, we have established that systems A, ASC, N, and L are integral in *trans*-1-amino-3-fluoro[1-^{14}C]cyclobutanecarboxylic acid (*anti*-[^{14}C]FACBC) uptake in human prostate cancer cell lines (Oka et al., 2012; Okudaira et al., 2011). However, the exact mechanisms of *anti*-[^{18}F]FACBC transport into glioma cells remain to be determined. Furthermore, although *anti*-[^{18}F]FACBC and [^{11}C]Met can image gliomas equally well in humans (Akhurst et al., 2006), differences in the mechanisms transporting these two tracers in gliomas have not been elucidated. In the present study, we set out to clarify the differences between the transport mechanisms for *anti*-[^{18}F]FACBC and [^{11}C]Met by using normal human astrocytes (NHA), low-grade (Hs683, SW1088), and high-grade (U87MG, T98G) human glioma cell lines (Kadowaki et al., 2012; Le Mercier et al., 2009) through a series of experiments, including time course experiment, pH dependency, competitive inhibition, exchange transport, and flow cytometry. Here, *anti*-[^{14}C]FACBC and L-[methyl-^{14}C]methionine ([^{14}C]Met), which differ from *anti*-[^{18}F]FACBC and [^{11}C]Met, respectively, only in the isotopes incorporated, were used as tracers, because the short half-lives of fluorine-18 and carbon-11 are impractical for *in vitro* study.

2. Results

2.1. Comparison between anti-[^{14}C]FACBC and [^{14}C]Met uptake in NHA and glioma cells

The time course of *anti*-[^{14}C]FACBC and [^{14}C]Met uptake was measured in NHA and glioma cell lines. As shown in Fig. 1, the uptake of *anti*-[^{14}C]FACBC was substantially higher than that of [^{14}C]Met in NHA and low-grade glioma cell lines (Hs683 and SW1088), and was almost equal to that of [^{14}C]Met in high-grade glioma cell lines (U87MG and T98G). Although significant differences between *anti*-[^{14}C]FACBC and [^{14}C]Met uptake were shown by 10 min in NHA, Hs683, and SW1088 cells, they were not seen until 30 or 60 min in U87MG and T98G cells. The intracellular amount of *anti*-[^{14}C]FACBC decreased moderately between 15 and 60 min in all cell lines, but [^{14}C]Met decreased only in SW1088 cells.

2.2. Ion dependency and pH dependency of anti-[^{14}C]FACBC and [^{14}C]Met uptake

Sodium, choline, and lithium buffers were used in this experiment because (1) all AATs work in sodium buffer, (2) only Na^+-independent AATs work in choline buffer, and (3) all Na^+-independent AATs and the Na^+-dependent N and y^+L AAT systems work in lithium buffer (Fei et al., 2000; Kanai et al., 2000; Nakanishi et al., 2001a, 2001b). Knowing this, the contributions of Na^+-dependent and Na^+-independent AATs to the uptake of *anti*-[^{14}C]FACBC and [^{14}C]Met into cells were estimated. If tracer uptake in choline or lithium buffer was higher than that in sodium buffer at each pH value, the contribution was recorded as 100%.

Figs. 2 and 3 show the changes in the contributions of Na^+-dependent and Na^+-independent AATs to the *anti*-[^{14}C]FACBC uptake in NHA and human glioma cell lines at acidic, neutral, and alkaline pH.

As shown in Fig. 2, the uptake of each tracer in sodium buffer at pH 7.3 was normalized to 100%. The intracellular amount of *anti*-[^{14}C]FACBC in sodium buffer at pH 7.3 was

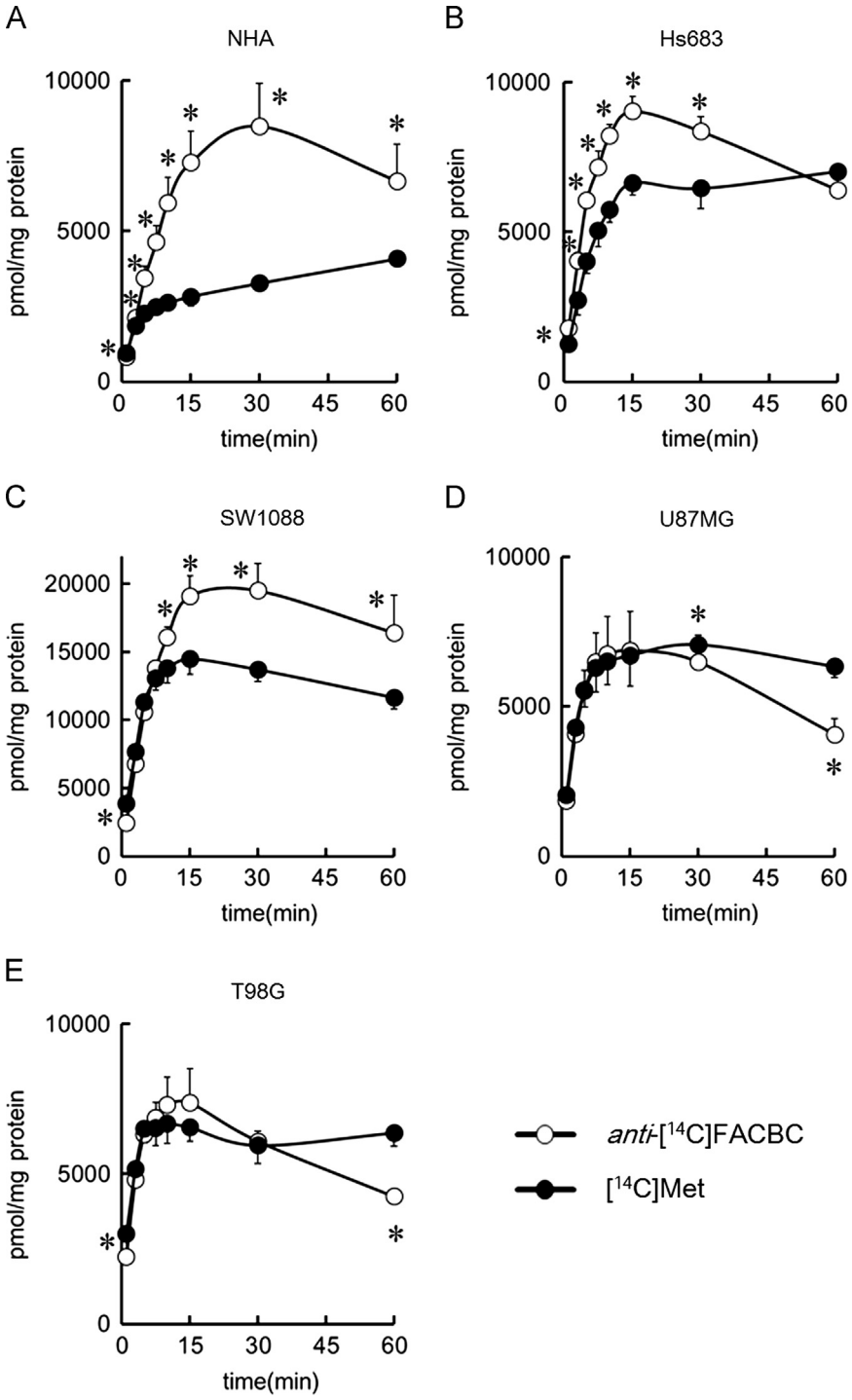

Fig. 1 – Time course of *anti*-[^{14}C]FACBC and [^{14}C]Met uptake in NHA and human glioma cell lines (Hs683, SW1088, U87MG, and T98G). Each point represents the mean ± SD ($n=6$). * $P<0.05$ *vs.* [^{14}C]Met.

significantly higher than that in choline and lithium buffers in all cell lines (3.6–36.8% and 6.4–40.8% of the uptake in sodium buffer at pH 7.3, respectively). At pH 6.0, the uptake of *anti*-[^{14}C]FACBC in sodium buffer dropped to 32.1–69.1%, whereas that in choline and lithium buffers increased to 10.0–58.4% and 9.2–56.8% compared with each buffer at pH 7.3, respectively. At pH 8.5, the uptake of *anti*-[^{14}C]FACBC in sodium buffer decreased to 83.4% and 80.6% in Hs683 and T98G, respectively, but not in the other cell lines. Furthermore, in NHA and T98G, the *anti*-[^{14}C]FACBC uptake dropped to 18.0% and 27.9% in choline buffer at pH 8.5, and to 20.7% and 31.8% in lithium buffer at pH 8.5, respectively, but not in the other cell lines. On the other hand, there was no significant difference for [^{14}C]Met uptake among each buffer at pH 7.3, except in NHA and Hs683 (90.4% and 56.3% in choline buffer, and 118% and 86.5% in lithium buffer, respectively). The [^{14}C]Met uptake at pH 6.0 was higher than that at pH 7.3, especially in choline buffer (111–169% that of the

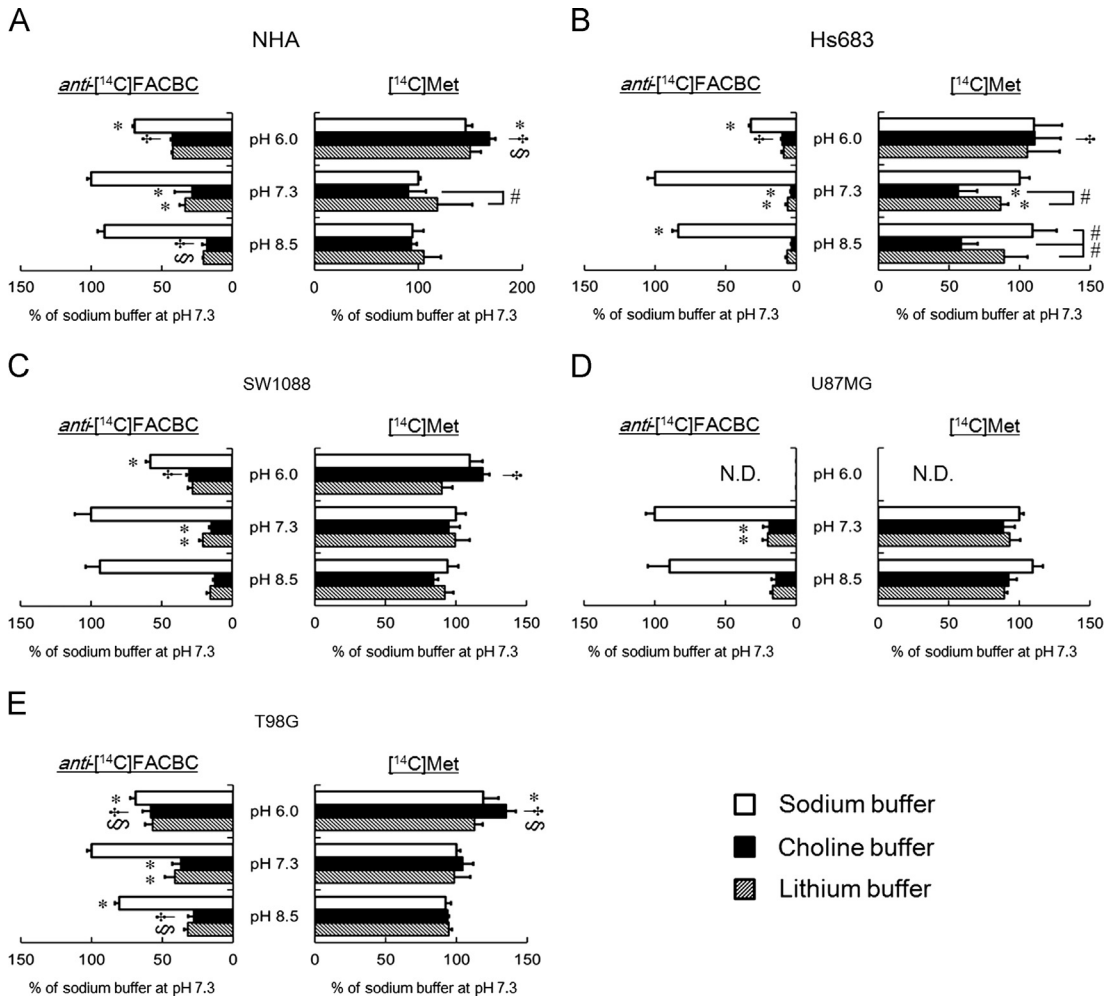

Fig. 2 – Ion and pH dependencies of *anti*-[^{14}C]FACBC uptake and [^{14}C]Met in NHA and human glioma cell lines (Hs683, SW1088, U87MG, and T98G). The percentage of uptake is expressed as the mean ± SD (n = 5–15). $^{*}P < 0.05$ *vs.* sodium buffer at pH 7.3; $^{\dagger}P < 0.05$ *vs.* choline buffer at pH 7.3; $^{\S}P < 0.05$ *vs.* lithium buffer at pH 7.3; $^{\#}P < 0.05$ *vs.* indicated bar; N.D.: not done, because U87MG detached from the culture plates at pH 6.0.

uptake in sodium buffer at pH 7.3). However, the intracellular amount of [^{14}C]Met at pH 8.5 was not changed in all the cell lines compared with that using each buffer at pH 7.3.

Furthermore, Fig. 3 shows the AAT contribution that was calculated from Fig. 2, using the formulas described in Section 4.4. In NHA at pH 7.3, Na^+-dependent and Na^+-independent AATs transported 71.5% and 28.5% of the total *anti*-[^{14}C]FACBC uptake, respectively. Similarly, the contributions of Na^+-dependent and Na^+-independent AATs to *anti*-[^{14}C]FACBC uptake were 96.4% and 3.6% in Hs683, 85.1% and 14.9% in SW1088, 80.8% and 19.2% in U87MG, and 63.2% and 36.8% in T98G, respectively. Thus, the contribution of the Na^+-dependent transport of *anti*-[^{14}C]FACBC tends to be higher in the low-grade oligodendroglioma cell line lines (Hs683, SW1088) than in the high-grade glioblastoma cell lines (U87MG, T98G). Among Na^+-dependent AATs, the contributions of the N and y^+L systems to *anti*-[^{14}C]FACBC transport were less than 5% in all cell lines. At pH 7.3, therefore, it would seem that Na^+-dependent AATs could transport *anti*-[^{14}C]FACBC except for the N and y^+L systems. On the other hand, the contributions of Na^+-dependent AATs for [^{14}C]Met uptake were 0.0–11.4% at the neutral pH in all cell types except for Hs683 (43.7%); the majority of the [^{14}C]Met uptake was mediated by Na^+-independent AATs (Hs683, 56.3%; others, 88.6–100%) (Fig. 3). Therefore, unlike *anti*-[^{14}C]FACBC uptake, Na^+-independent AATs were largely responsible for [^{14}C]Met uptake at pH 7.3.

It is reported that transport activity via system L is facilitated in acidic conditions, while that via system N is diminished (Fei et al., 2000; Nakanishi et al., 2001a, 2001b). As shown in Figs. 2 and 3, the transport of *anti*-[^{14}C]FACBC and [^{14}C]Met via Na^+-independent AATs was facilitated at pH 6.0 in all cell lines except U87MG, while the uptake profiles of the both tracers were almost unchanged in the alkaline condition. These results support the idea that system L mediates the transport of *anti*-[^{14}C]FACBC and [^{14}C]Met.

2.3. *Competitive inhibition transport assay*

To narrow down the AATs involved in *anti*-[^{14}C]FACBC and [^{14}C]Met uptake, the inhibitory effects of synthetic/naturally-occurring amino acids on tracer uptake were investigated.

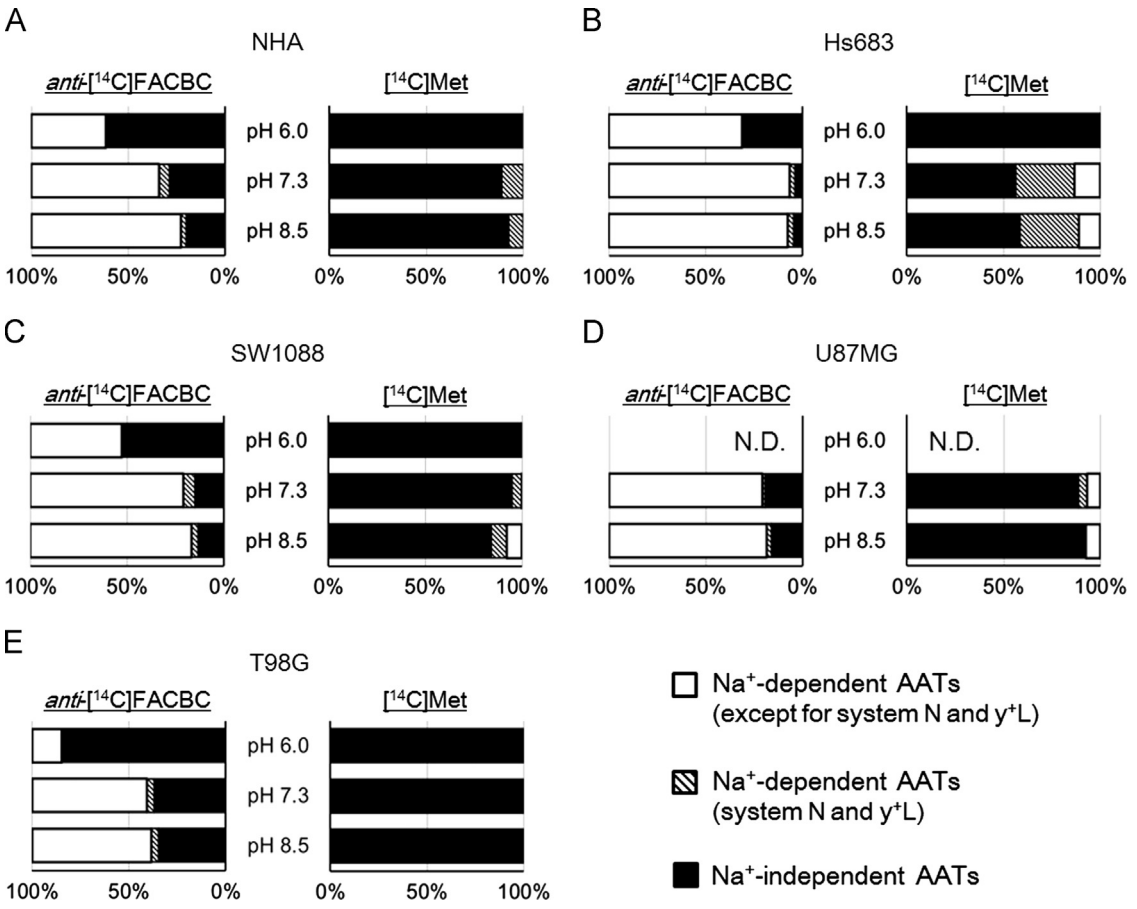

Fig. 3 – AAT contribution percentages of *anti*-[^{14}C]FACBC and [^{14}C]Met uptake in NHA and human glioma cell lines (Hs683, SW1088, U87MG, and T98G). The mean contribution of AATs in each buffer was calculated from Fig. 2, using the formulas in Section 4.4 (n=5–15). N.D.: not done, because U87MG detached from the culture plates at pH 6.0.

Intensity of inhibition was categorized into four classes based on the average inhibitory rates: null (<20%), weak (20–49.9%), moderate (50–79.9%) and strong (≥80%).

As shown in Fig. 4A–D, null to weak inhibitory effects by 2 mM 2-(methylamino)-isobutyric acid (MeAIB, a substrate for systems A, IMINO, and PAT), L-arginine (Arg, a substrate for systems $B^{0,+}$, y^+L, $b^{0,+}$, and y^+), L-glutamate (Glu, a substrate for systems X^-_C and $X^-_{A,G}$), and L-proline (Pro, a substrate for systems A, ASC [ASCT1], G-like, IMINO, B^0 [B^0AT2], $B^{0,+}$, and PAT) were observed on the uptake of *anti*-[^{14}C]FACBC and [^{14}C]Met in sodium and choline buffers. There were no inhibitory effects on the transport of either tracer if MeAIB and Arg were employed as inhibitors, even at high concentration (5 or 10 mM) (data not shown). These results suggest that the contributions of AATs, including systems A, IMINO, PAT, $B^{0,+}$, y^+L, $b^{0,+}$, y^+, X^-_C, and/or $X^-_{A,G}$, to the transport of *anti*-[^{14}C]FACBC and [^{14}C]Met are low. In the absence of Na^+, L-phenylalanine (Phe, a substrate for systems L and T) and 2-amino-bicyclo[2,2,1] heptane-2-carboxylic acid (BCH, a substrate for system L) showed strong inhibitory effects on the uptake of *anti*-[^{14}C] FACBC and [^{14}C]Met in all cell lines (Fig. 4C and D). Moreover, *N*-ethylmaleimide (NEM), a substrate for systems y^+ and L (except LAT1), induced weak to moderate inhibition of *anti*-[^{14}C]FACBC and [^{14}C]Met uptake only in Hs683, with or without Na^+ (Fig. 4A–D). Therefore, it is possible that within system L, LAT1 is involved mainly in the transport of *anti*-[^{14}C]FACBC and [^{14}C]Met in all cell lines, while the other subtypes of system L (LAT2, 3, and/or 4), except for LAT1, also contribute to *anti*-[^{14}C]FACBC and [^{14}C]Met uptake in Hs683. Although the contribution of system T to *anti*-[^{14}C]FACBC and [^{14}C]Met uptake should be considered in light of the inhibitory effects of Phe, its contribution is unexpected because system T selectively transports aromatic amino acids (*e.g.* Phe, L-tryptophan, and L-tyrosine) (SLC tables, 2013, see *"References"*), and *anti*-[^{14}C] FACBC and [^{14}C]Met do not possess an aromatic ring.

In the presence of Na^+, both L-glutamine (Gln) and L-serine (Ser), which are preferentially transported by systems A, ASC (especially ASCT2 for Gln transport), B^0 (B^0AT1), N, y^+L, L, asc, and/or $B^{0,+}$, showed the strongest inhibitory effect on *anti*-[^{14}C] FACBC uptake in all cell lines (Fig. 4A). In contrast, although [^{14}C]Met uptake was inhibited strongly by Gln in sodium buffer in all cell lines except for Hs683, the inhibitory effect of Ser was weak to moderate in all cell lines, except T98G (Fig. 4B). The results so far narrow down the AATs involved in transport of *anti*-[^{14}C]FACBC and [^{14}C]Met to systems ASC (especially ASCT2), B^0 (especially B^0AT1), N, L, and asc. However, because previous studies reported that expression of systems B^0 and asc cannot be detected in astrocytes (Bröer, 2006; Shao et al., 2009), the contributions of systems B^0 and asc to *anti*-[^{14}C]FACBC and [^{14}C] Met transport could be negligible.

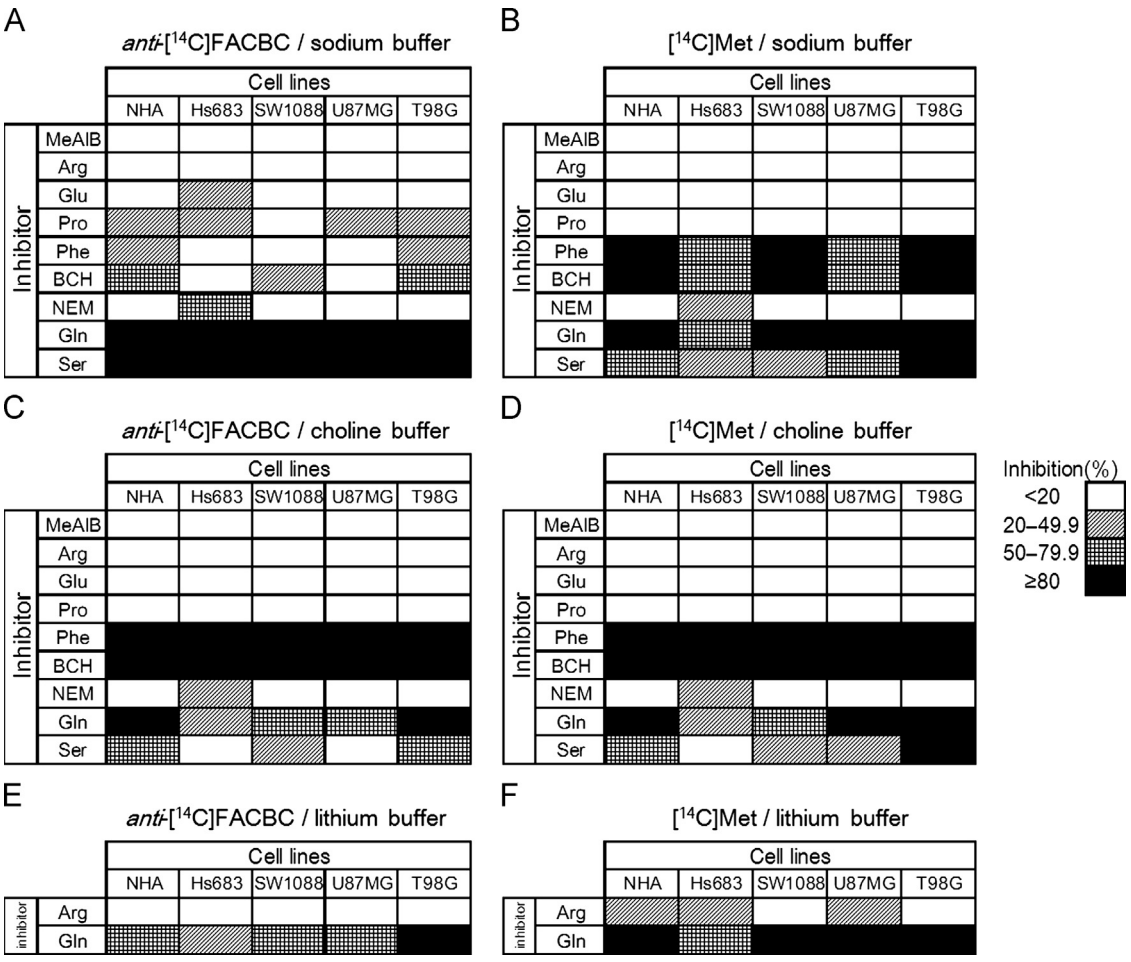

Fig. 4 – Competitive inhibition profiles of NHA and human glioma cell lines (Hs683, SW1088, U87MG, and T98G) on *anti*-[^{14}C]FACBC and [^{14}C]Met. Incubation of *anti*-[^{14}C]FACBC (A, C, E) or [^{14}C]Met (B, D, F) in sodium (A, B), choline (C, D), or lithium (E, F) buffer with the indicated amino acids (2 mM). The average inhibitory rates (n=5–9) were categorized into 4 classes.

In lithium buffer, the inhibitory effects of Arg and Gln on the uptake of [^{14}C]Met were strong compared with those on *anti*-[^{14}C]FACBC, that is, systems N and y^+L mediate the uptake of [^{14}C]Met rather than that of *anti*-[^{14}C]FACBC. The contributions of these AATs on the uptake of both tracers may be insignificant, however, because Li^+-dependent transport of *anti*-[^{14}C]FACBC and [^{14}C]Met was a small proportion of the total uptake of either tracer (Figs. 2 and 3).

In NHA, the overall tendencies in the inhibitory effects of synthetic and naturally occurring amino acids on *anti*-[^{14}C]FACBC and [^{14}C]Met uptake were similar to those in SW1088. Because both cells are from an astroglial lineage, similarities in the transport of *anti*-[^{14}C]FACBC and [^{14}C]Met imply the properties are tissue specific in nature.

Taken together with the results listed in Section 2.2 (Figs. 2 and 3), the ASC and L systems, especially ASCT2 and LAT1, could be central players in the transport of *anti*-[^{14}C]FACBC, while system L is the critical AAT for [^{14}C]Met uptake.

2.4. *Tracer exchange transport*

The ASC and L (LAT1 and LAT2) systems are amino acid exchangers that exchange their intracellular and extracellular substrates (SLC tables, 2013, see "*References*"). To confirm that these AATs are responsible for *anti*-[^{14}C]FACBC and [^{14}C]Met transport, we conducted exchange transport studies. The results at 37 °C and 4 °C in the absence of synthetic or naturally occurring amino acids indicated active and passive diffusion, respectively.

As shown in Fig. 5A, without amino acids, 31.9% of the intracellular *anti*-[^{14}C]FACBC in NHA was effluxed in 13 min at 37 °C, and this dropped to 12.9% at 4 °C. The corresponding values for the other cell lines were 19.3–62.0% and 10.0–16.2% at 37 °C and 4 °C, respectively (Fig. 5B–E). Similar results were observed for [^{14}C]Met efflux in the absence of amino acids (efflux at 13 min: 27.0–67.3% at 37 °C and 7.2–16.2% at 4 °C) (Fig. 6), indicating that the active diffusion rates varied between the cells used in this study, while the passive diffusion rates did not.

When Gln or BCH was added to the sodium buffer, *trans*-stimulation of *anti*-[^{14}C]FACBC efflux was observed in all cell lines, with Gln having the greater effect (after 13 min: Gln 93.0–98.2% *vs.* BCH 56.5–74.3%) (Fig. 5). Along with *anti*-[^{14}C]FACBC efflux, the addition of Gln or BCH to the sodium buffer caused *trans*-stimulation of [^{14}C]Met efflux, with the degree of stimulation at the 13-min point being almost same in all cell

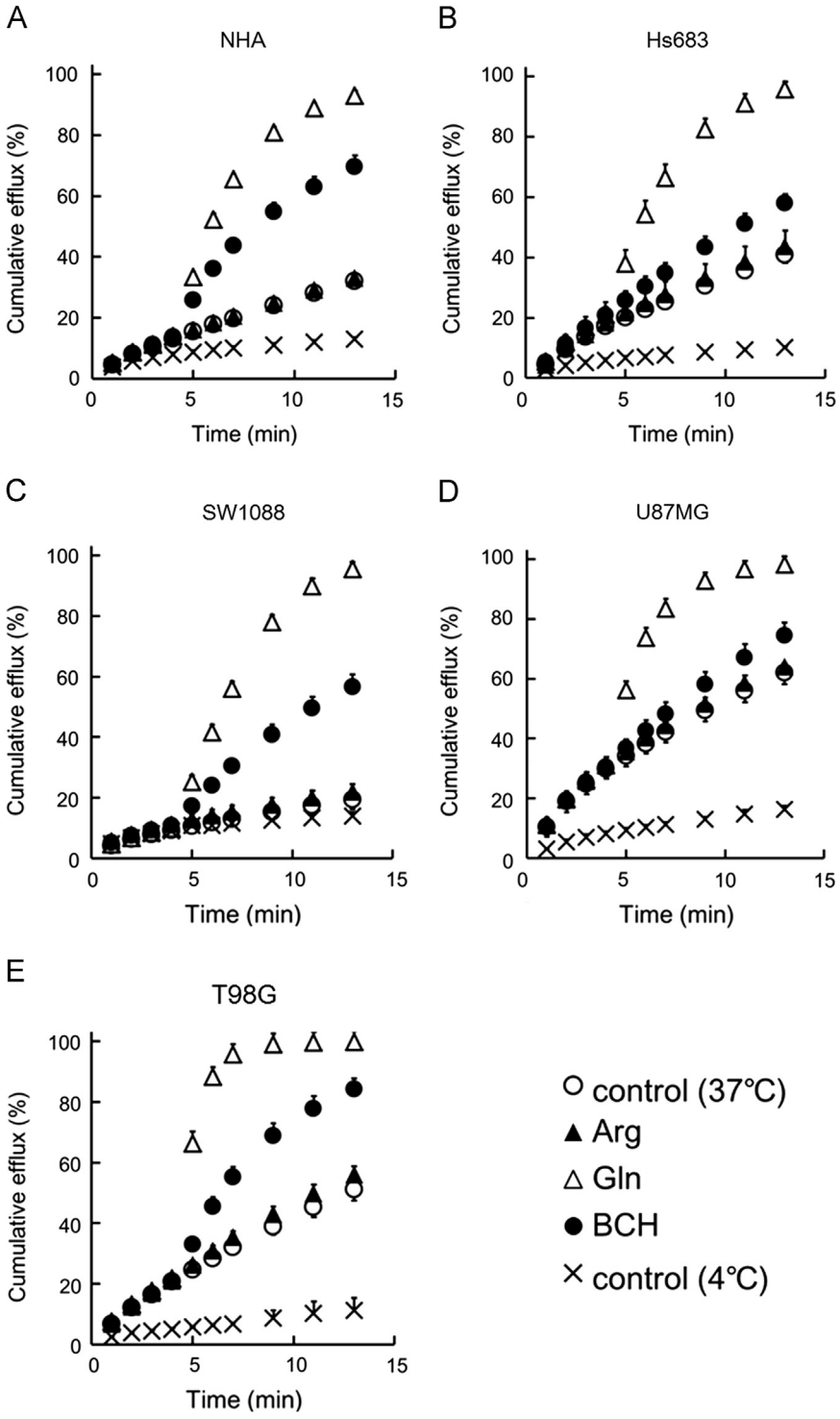

Fig. 5 – Exchange transport of *anti*-[^{14}C]FACBC in NHA and human glioma cell lines (Hs683, SW1088, U87MG, and T98G) in sodium buffer. At the 4-min point, the indicated amino acids (2 mM) were added. Each point represents the mean ± SD (n = 3–6).

lines (Gln, 76.9–89.0%; BCH, 74.3–88.7%) (Fig. 6). Arg had no *trans*-stimulating effect on *anti*-[^{14}C]FACBC or [^{14}C]Met efflux in any cell line (Figs. 5 and 6).

As shown in Fig. 7, in the absence of Na^+ in Hs683 and T98G, the efflux without inhibitor at 13 min for *anti*-[^{14}C]FACBC was 50.8% and 40.3%, respectively, at 37 °C, and this decreased to 8.5% and 6.0%, respectively, at 4 °C (Fig. 7A and C). Similar tendencies for [^{14}C]Met were observed at 13 min in Hs683 and T98G (42.8% and 29.5% at 37 °C, and 7.1% and 5.2% at 4 °C, respectively; Fig. 7B and D). In the presence of Gln or BCH, *trans*-stimulation of the *anti*-[^{14}C]FACBC and [^{14}C]Met effluxes was observed in Hs683 and T98G. Unlike the efflux in sodium buffer, the efflux degrees were almost equal in each tracer (*anti*-[^{14}C]FACBC efflux at 13 min in Hs683 and

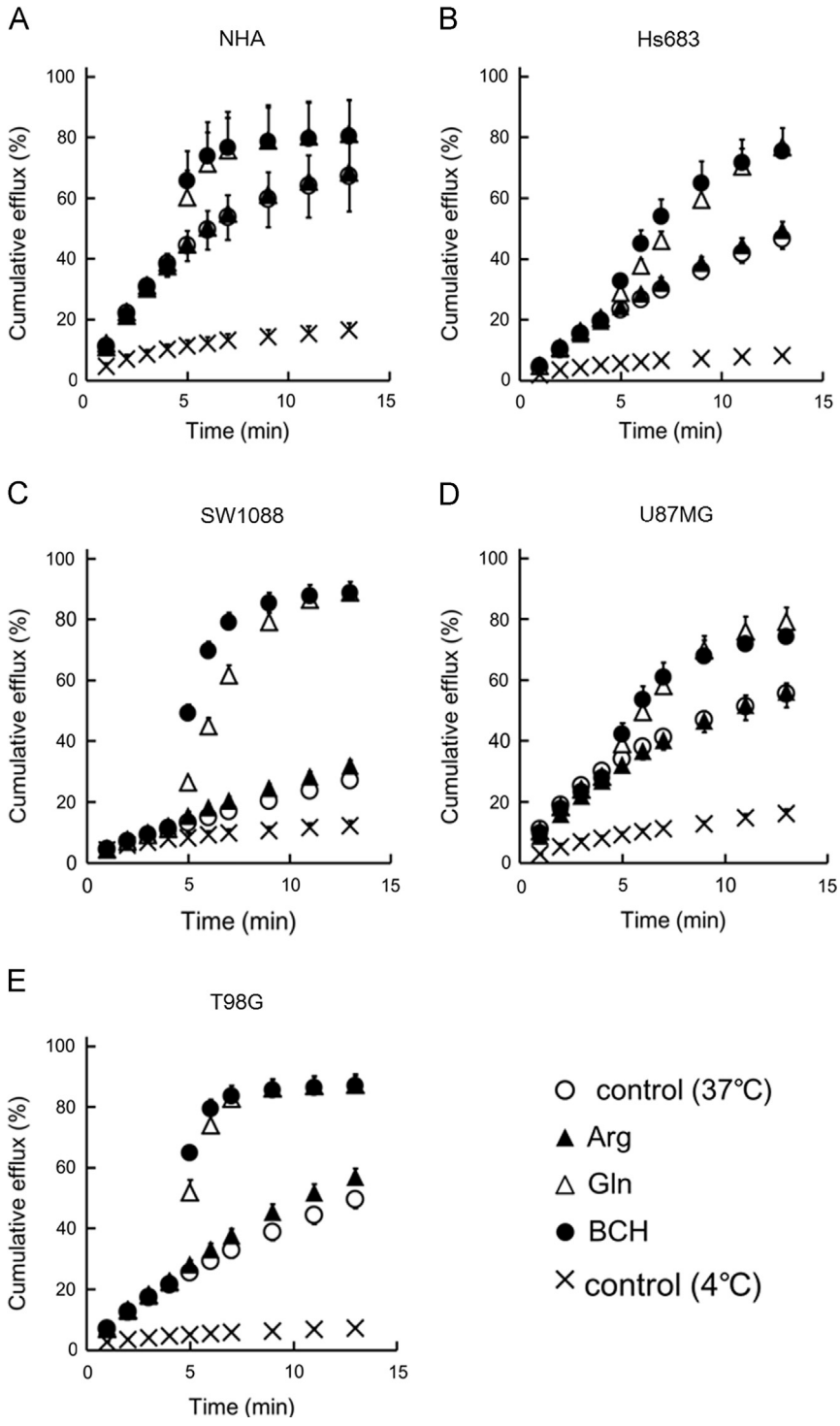

Fig. 6 – Exchange transport of [^{14}C]Met in NHA and human glioma cell lines (Hs683, SW1088, U87MG, and T98G) in sodium buffer. At the 4-min point, the indicated amino acids (2 mM) were added. Each value represents the mean ± SD (n = 3–6).

T98G: Gln 62.9% and 99.2% *vs.* BCH 71.3% and 94.4%, respectively; [^{14}C]Met efflux at 13 min in Hs683 and T98G: Gln 68.0% and 86.7% *vs.* BCH 71.9% and 85.9%, respectively) (Fig. 7).

Considering that (1) Gln has affinity for the ASC (especially ASCT2), N, L, y^+L, asc and $b^{0,+}$ systems; (2) Arg is a representative substrate for the y^+L and $b^{0,+}$ systems, and; (3) BCH is exclusively recognized by system L, a review of the *trans*-stimulation effects in all cell lines suggests that *anti*-[^{14}C]FACBC is mainly transported *via* the ASC and L systems, while the L system predominates in [^{14}C]Met transport, as described in Section 2.3.

2.5. *AAT expression in NHA and glioma cell lines*

The expression profiles of ASCT1, ASCT2, LAT1, and 4F2 heavy chain (4F2hc, a regulatory subunit of LAT1) in NHA

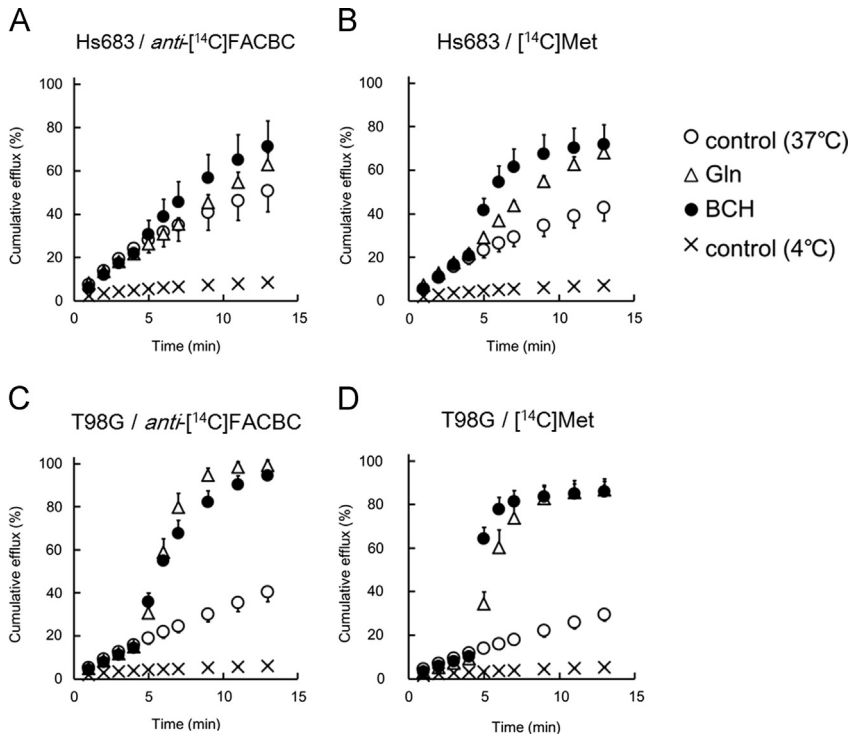

Fig. 7 – Exchange transport of *anti*-[^{14}C]FACBC and [^{14}C]Met in human glioma cell lines (Hs683 and T98G) in choline buffer. At the 4-min point, the indicated amino acids (2 mM) were added. Each value represents the mean ± SD (n = 3–9).

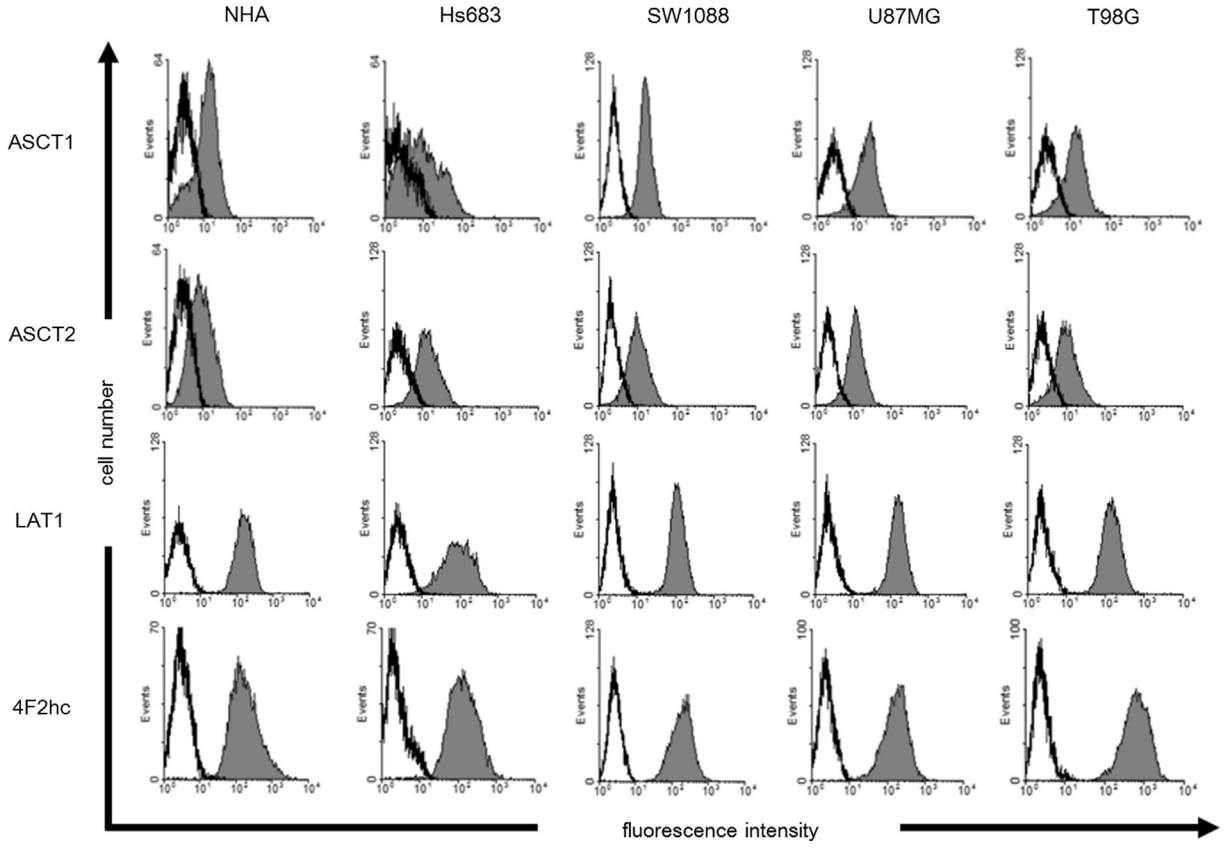

Fig. 8 – AAT expression profile of NHA and human glioma cell lines (Hs683, SW1088, U87MG, and T98G). Fluorescence intensity (horizontal axis) and cell number (vertical axis) were analyzed using a flow cytometer. Each histogram represents the fluorescence intensity of AAT expression (closed histogram) and isotype control (open histogram), respectively (n = 3).

and glioma cell lines were analyzed using flow cytometry. As shown in Fig. 8, the three AAT subtypes and 4F2hc were expressed in all cell lines.

3. Discussion

We set out to determine the differences between the transport mechanisms for *anti*-[^{14}C]FACBC and [^{14}C]Met in NHA and human glioma cell lines by several *in vitro* experiments, including time-course experiments, Na^+ dependency, pH dependency, competitive inhibition, and exchange transport. First, we found that the uptake of *anti*-[^{14}C]FACBC was substantially higher than that of [^{14}C]Met in NHA and low-grade glioma cell lines (Hs683, SW1088), but was almost equal to that of [^{14}C]Met in high-grade glioma cell lines (U87MG and T98G: glioblastoma). Akhurst et al. (2006) reported that the accumulation rate of *anti*-[^{18}F]FACBC in glioblastoma and high-grade astrocytoma is faster than that of [^{11}C]Met, and that the ratio of tumor-to-normal brain accumulation is higher with *anti*-[^{18}F]FACBC than with [^{11}C]Met. Furthermore, PET imaging with [^{11}C]Met has the potential to visualize not only high-grade but also low-grade gliomas (Herholz et al., 1998). Therefore, our results suggest that *anti*-[^{18}F]FACBC as well as [^{11}C]Met would be expected to be effective in visualization, evaluation, and follow up for low-grade gliomas.

Second, we showed that the Na^+-dependent ASC system (especially ASCT2) and the Na^+-independent L system (especially LAT1) play a central role in *anti*-[^{14}C]FACBC transport, and that the L system (especially LAT1) is mainly involved in [^{14}C]Met transport in NHA and glioma cell lines. We also used flow cytometry to confirm that ASCT2, LAT1, and 4F2hc are expressed in all the cell lines. These results are in accord with the results from our previous studies, which included an ASCT2-silenced transport study using human prostate cancer cell lines (Oka et al., 2012; Okudaira et al., 2011), as well as with the results from the kinetic assay for ASCT2 and LAT1 (Okudaira et al., 2013) and the results of others (Kanai et al., 1998; Yu et al., 2009). The fact that *anti*-[^{14}C]FACBC is a substrate for both the ASC and L systems is not surprising because naturally occurring amino acids are transported into cells by more than one transport system, and ASCT2 and LAT1 share several substrates, such as L-threonine, L-leucine, and L-phenylalanine. Furthermore, the recognition of *anti*-[^{14}C]FACBC by both systems might lead to its higher uptake as compared with [^{11}C]Met, because ASCT2 and LAT1 are up-regulated in brain tumor cells (Fuchs and Bode, 2005), and there are thus two routes for *anti*-[^{14}C]FACBC transport compared with one for [^{14}C]Met. Indeed, the uptake of *anti*-[^{14}C]FACBC in some glioma cell lines was higher than that of [^{14}C]Met, as described in Section 2.1.

While the ASC and L systems are involved in the transport of *anti*-[^{14}C]FACBC in glioma and prostate cancer cells, a Na^+-dependent system A, which participates in *anti*-[^{14}C]FACBC uptake in prostate cancer cell lines (Okudaira et al., 2011), is not involved in the transport of *anti*-[^{18}F]FACBC in glioma cells, because MeAIB, a specific inhibitor of system A, showed no inhibitory effect on *anti*-[^{14}C]FACBC uptake in this study (Fig. 4). The difference between prostate cancer and glioma cells may be attributed to the fact that the expression of system A in glioma cells is at a lower level than in prostate cancer cells. In fact, it is reported that system A is abundant in prostate cancer cells (Okudaira et al., 2011), but poorly expressed in astrocytes (Mackenzie and Erickson, 2004), and that all cell lines used in the current study are derived from glial cells. We therefore suggest that the main AATs for the transport of *anti*-[^{18}F]FACBC are the ASC and L systems, while system L is mainly responsible for [^{11}C]Met transport. System L transports both tracers into cells regardless of their tissue source and/or malignancy, whereas the contributions of other AATs such as systems A and N vary by cell type.

The transport activities of systems N and y^+L are unaffected by the substitution of Li^+ for Na^+ (Fei et al., 2000; Kanai et al., 2000; Nakanishi et al., 2001a, 2001b). [^{14}C]Met transport in Hs683 is Li^+ tolerant at pH 7.3 and 8.5, indicating the contribution of the N and y^+L systems is higher (approximately 30%) than in other cell lines (Figs. 2 and 3). Moreover, the inhibition study on [^{14}C]Met uptake in the presence of Li^+ (Fig. 4F) showed moderate inhibition by Gln, a substrate for system N, but not by Arg, a substrate for system y^+L. These results suggest that system N is partly involved in [^{14}C]Met transport in Hs683, a low-grade glioma cell line. Sidoryk et al. (2004) reported that the expression of SNAT3, a subtype of system N, is increased in gliomas. Thus, it is possible that system N mediates a portion of the [^{11}C]Met transport in low-grade gliomas, and this is a reason why they can be detected by [^{11}C]Met-PET (Herholz et al., 1998). However, system N cannot be an important AAT in [^{11}C]Met transport in advanced high-grade gliomas because the pH microenvironment in progressive tumor tissue is relatively acidic (Zhang et al., 2010), and the activity of system N is inhibited by low pH (Fei et al., 2000; Nakanishi et al., 2001a, 2001b). The results of the current study support these conclusions.

The exchange transport study showed that, apart from U87MG, it might be possible to correlate differences in the efflux rates of *anti*-[^{14}C]FACBC and [^{14}C]Met between 37 °C and 4 °C with the total tracer uptake. For example, the differences in SW1088 were smaller than in the other cell lines (Figs. 5 and 6), and the uptake of both tracers was higher (Fig. 1). These findings suggest that the total amounts of *anti*-[^{14}C]FACBC and [^{14}C]Met in cells were regulated by efflux activity rather than influx activity.

Contrary to our expectations, the total uptake of *anti*-[^{14}C]FACBC, but not [^{14}C]Met, in NHA was relatively high compared to that in glioma cell lines (Fig. 1A). It was reported in a clinical study, however, that *anti*-[^{18}F]FACBC accumulation in normal brain tissue is low, but is constantly high in a glioma (Shoup et al., 1999). A possible explanation for this discrepancy between our *in vitro* experiments and the clinical study is as follows: as described in Section 2.3, Gln was one of the most effective inhibitors of *anti*-[^{14}C]FACBC uptake in the presence of Na^+, and ASCT2 is thought to be the main AAT for Gln and *anti*-[^{14}C]FACBC. It is known that Gln and ASCT2 are indispensable for cell growth, and that Gln itself has the potential to enhance ASCT2 expression on the surface of astrocytes by inducing the trafficking of ASCT2 from the cytoplasm (Bode et al., 2002; Bröer and Brookes, 2001; Gegelashvili et al., 2006). Furthermore, Bröer et al. (1999) reported that ASCT2 expression in cultured rat astrocytes is much higher than that in the adult brain. Considering the

transport mechanism of *anti*-[^{14}C]FACBC into cells, it is reasonable to increase the transport of *anti*-[^{14}C]FACBC in NHA.

As mentioned above, it is reported that the accumulation of *anti*-[^{18}F]FACBC in normal brain tissue is lower than that of [^{11}C]Met; the standard uptake values of *anti*-[^{18}F]FACBC and [^{11}C]Met in the cortex of human brain were 0.5 ± 0.1 and 1.3 ± 0.4, respectively (Akhurst et al., 2006). One reason for the low accumulation of *anti*-[^{18}F]FACBC in the normal brain is that *anti*-[^{18}F]FACBC is not metabolized and incorporated into protein (Okudaira et al., 2011). According to a report by O'Kane et al., (2004), Na^+-dependent AATs, including the A, N, and ASC systems, are expressed on the abluminal blood–brain-barrier (BBB) membrane, while LAT1 is present on the abluminal membrane, but is predominantly on the luminal membrane. The presence of Na^+-dependent AATs on the abluminal BBB membrane provides a mechanism by which neutral amino acid concentrations in the extracellular brain fluid are maintained at <10% of those of plasma (Laterra et al., 1999; O'Kane et al., 2004). Thus, it might be speculated that a small accumulation of *anti*-[^{18}F]FACBC in the normal brain is related to the removal of neutral amino acids via Na^+-dependent AATs such as system ASC on the abluminal membrane.

In conclusion, we elucidated the differences in transport mechanisms between *anti*-[^{14}C]FACBC and [^{14}C]Met in NHA and human glioma cell lines. Our results demonstrate that uptake of *anti*-[^{14}C]FACBC was higher than that of [^{14}C]Met in low-grade glioma cell lines, and was almost equal to that of [^{14}C]Met in high-grade glioma cell lines. Furthermore, ASC systems (especially ASCT2) as well as L systems (especially LAT1) play a central role in *anti*-[^{14}C]FACBC transport, while L systems (especially LAT1) are predominantly involved in [^{14}C]Met transport in NHA and glioma cell lines. Because our results were obtained from *in vitro* experiments, further investigations are necessary to determine if these mechanisms operate *in vivo*.

4. Experimental procedure

4.1. Radioisotope-labeled tracers

In all experiments, ^{14}C-labeled amino acids were used because their long half-lives (5700 years) made them more convenient for *in vitro* experiments than ^{18}F (110 min) or ^{11}C (20 min). *Trans*-1-amino-3-fluoro[1-^{14}C]cyclobutanecarboxylic acid (*anti*-[^{14}C]FACBC, 2.09 GBq/mmol) was synthesized (Oka et al., 2012) by Sekisui Medical Co., Ltd. (Tokyo, Japan), and L-[methyl-^{14}C]methionine ([^{14}C]Met, 2.04 GBq/mmol) was purchased from American Radiolabeled Chemicals (Missouri, USA).

4.2. Cell culture

Human glioma-derived cell lines Hs683 (low-grade oligodendroglioma), SW1088 (low-grade astrocytoma), U87MG (high-grade glioblastoma), and T98G (high-grade glioblastoma) (Kadowaki et al., 2012; Le Mercier et al., 2009) were obtained from the American Type Culture Collection (Maryland, USA). Dulbecco's modified Eagle Medium (DMEM), Leibovitz's L-15 Medium (L-15), Minimum Essential Medium (MEM), and penicillin–streptomycin were purchased from Life Technologies Japan (Tokyo, Japan). Cells were maintained in DMEM (Hs683), L-15 (SW1088), or MEM (U87MG and T98G) at 37 °C in air (SW1088) or 5% CO_2 (Hs683, U87MG and T98G). All media were supplemented with 10% fetal bovine serum (FBS), 100 units/mL penicillin, and 0.1 mg/mL streptomycin. Normal human astrocytes (NHA) were purchased from Takara Bio Inc. (Shiga, Japan) and cultured under 5% CO_2 in astrocyte basal medium supplement with FBS, epidermal growth factor, ascorbic acid, Gln, gentamicin, and amphotericin B, according to the manufacturer's protocol.

4.3. Time-dependent uptake study

All reagents used in the current study were purchased from commercial suppliers (Wako Pure Chemical Industries, Osaka, Japan; Sigma-Aldrich Japan, Tokyo, Japan; and Nacalai Tesque, Kyoto, Japan) unless otherwise noted. Cells were seeded at densities of 3×10^4 (SW1088), 5×10^4 (Hs683 and T98G), or 7.5×10^4 (NHA and U87MG) cells per well in 24-well flat-bottom tissue culture plates (Becton Dickinson, New Jersey, USA). After 3 days of cultivation, the cells were washed twice with sodium buffer (140 mM NaCl, 5 mM KCl, 5.6 mM D-glucose, 0.9 mM $CaCl_2$, 1 mM $MgCl_2$, and 10 mM HEPES, pH 7.3 at 37 °C), and then incubated with 0.3 mL of sodium buffer containing *anti*-[^{14}C]FACBC or [^{14}C]Met at a final concentration of 10 μM for 1, 3, 5, 7.5, 10, 15, 30, and 60 min at 37 °C in air. The uptake was terminated by removing the tracer solution and rapidly washing the cells twice with ice-cold sodium buffer. The cells were lysed in 0.3 mL of 0.1 N NaOH, and the radioactivity of each aliquot was measured with a Tri-Carb 2910 TR liquid scintillation counter (PerkinElmer, Massachusetts, USA) by using Ultima Gold (PerkinElmer). The protein concentration of the cell lysate was determined with a VersaMax microplate reader (Nihon Molecular Device K.K., Osaka, Japan) using the BCA Protein Assay Kit (Thermo Fisher Scientific, Kanagawa, Japan). Tracer uptake was expressed as pmol/mg protein.

4.4. Study of ion-dependent and pH-dependent uptake

Experiments were carried out as described previously (Oka et al., 2012) with minor modifications. Sodium, choline, and lithium buffers were used in this study. In choline and lithium buffers, sodium chloride was replaced by the equivalent concentrations of choline chloride and lithium chloride, respectively. The pH of the buffers was adjusted to 6.0 or 8.5, as follows: HEPES was replaced with the equivalent concentration of either 4-morpholineethanesulfonic acid (for pH 6.0) or Tris (for pH 8.5).

Cells were cultured as described above. After washing twice with sodium, choline, or lithium buffer at each pH, cells were incubated with each buffer containing *anti*-[^{14}C]FACBC or [^{14}C]Met at a final concentration of 10 μM for 5 min at 37 °C in air. The radioactivity and protein concentration of each sample were measured as described above. The data from U87MG at pH 6.0 were not determined because this cell line was easily detached from the tissue culture plate during the cell washing procedure.

In this experiment, all AATs functioned in sodium buffer, while only Na^+-independent AATs worked in choline buffer. In lithium buffer, both Na^+-independent AATs and the Na^+-dependent N and y^+L systems worked (Fei et al., 2000; Kanai et al., 2000; Nakanishi et al., 2001a, 2001b). From this knowledge, the amounts of tracer uptake (pmol/mg protein) mediated by each amino acid transport system were calculated as follows:

Na^+-independent AATs $= V_C$
Na^+-dependent AATs $= V_S - V_C$ (1)
System N and y^+L AATs $= V_L - V_C$ (2)
Na^+-dependent AATs except for system N and y^+L AATs = (1) − (2)

where V_S, V_C, and V_L are the amounts of tracer uptake in sodium, choline, and lithium buffers, respectively. In Fig. 2, the amount of each tracer uptake in sodium buffer at pH 7.3 was normalized to 100%. In Fig. 3, the transport of tracers in sodium buffer at each pH was normalized to 100%. If the tracer uptake in choline buffer was higher than that in sodium buffer at each pH, then the contribution of Na^+-dependent AATs was taken to be zero. If the tracer uptake in lithium buffer was higher than that in sodium buffer at each pH, then the uptake in lithium buffer was considered same as that in sodium buffer.

4.5. *Competitive inhibition uptake study*

Experiments were carried out as described previously (Oka et al., 2012) with minor modifications. Cells in 24-well flat-bottom tissue culture plates were incubated in sodium, choline, or lithium buffer containing 10 μM *anti*-[^{14}C]FACBC or [^{14}C]Met for 5 min at 37 °C in air in the presence or absence of 2 mM inhibitors. As inhibitors, synthetic and naturally occurring amino acids were used as follows: 2-amino-bicyclo[2,2,1] heptane-2-carboxylic acid (BCH, for system L, B^0, and $B^{0,+}$); 2-(methylamino)-isobutyric acid (MeAIB, for system A, IMINO and PAT); N-ethylmaleimide (NEM, for system y^+ and LAT2/3/4); L-phenylalanine (Phe, for system L, T); L-proline (Pro, for system A, ASC [ASCT1], G-like, IMINO, B^0, $B^{0,+}$, and PAT); L-glutamine (Gln, for system A [SNAT1, SNAT2], ASC [ASCT2], B^0 [B^0AT1], N, y^+L, L, and $B^{0,+}$); L-serine (Ser, for system A, ASC, B^0 [(B^0AT1]), N [(SNAT5]), y^+L, L, and $B^{0,+}$); L-arginine (Arg, for system $B^{0,+}$, y^+L, $b^{0,+}$, and y^+); and L-glutamate (Glu, for system X^-_C, $X^-_{A,G}$). Following that, the procedures were carried out as described above.

In data analyses, the control transport of *anti*-[^{14}C]FACBC and [^{14}C]Met in sodium, choline, and lithium buffers was normalized to 100%, and the inhibitory effects of the synthetic and naturally occurring amino acids on the uptake of both tracers were calculated as a percentage of the control. To simplify the results, the intensity of the inhibitory effects was categorized into 4 classes based on the average inhibitory rates: null (<20%), weak (20–49.9%), moderate (50–79.9%), and strong (≥80%). A summary of these profiles is shown in Fig. 4.

4.6. *Tracer efflux study*

This study was performed as described previously (Oka et al., 2012). Cells were cultured in 35-mm cell culture dishes (Becton Dickinson) and loaded with *anti*-[^{14}C]FACBC or [^{14}C]Met in sodium or choline buffer (final concentration: 10 μM) for 15 min at 37 °C in air. After 2 quick washes with ice-cold sodium or choline buffer, cells were added to 0.5 mL of sodium or choline buffer and incubated at 37 °C in air. The efflux of each tracer from the cells was measured by the sequential addition and removal of 0.5 mL of buffer at every minute until 3 min. At the 4-min point, each warmed sodium buffer (37 °C) with or without 2 mM Arg, Gln, or BCH, or warmed choline buffer (37 °C) with or without 2 mM Gln or BCH was added to the dishes, and the buffer exchange was repeated at the 5-, 6-, 7-, 9-, 11-, and 13-min time points. In some experiments, ice-cold sodium or choline buffer without inhibitors was used in the buffer-exchange procedures. The radioactivity of the collected buffer and the cell lysate was measured as described above.

4.7. *Flow cytometry*

Anti-LAT1 monoclonal antibody (clone 181C, mouse IgG1 mAb) was kindly provided by Dr. Tsurudome (Mie University) (Okamoto et al., 2002). Anti-ASCT1 polyclonal antibody (rabbit IgG pAb) was purchased from Medical & Biological Laboratories (Nagoya, Japan). Anti-ASCT2 rabbit pAb was obtained from Santa Cruz Biotechnology (California, USA). Anti-human 4F2hc phycoerythrin (PE)-labeled monoclonal antibody (mouse IgG1 mAb) was purchased from Becton Dickinson. Purified mouse IgG1 (Becton Dickinson) and purified rabbit IgG (Beckman) were used as isotype controls. PE-labeled anti-mouse IgG1 (rat IgG1; Becton Dickinson) and PE-labeled anti-rabbit IgG (goat IgG; Santa Cruz Biotechnology) were used as secondary antibodies. The staining of cells with antibodies was performed as described previously (Oka et al., 2012) and data were acquired using a FACSCalibur flow cytometer (Becton Dickinson).

4.8. *Statistical analysis*

All data are presented as the mean ± standard deviation (SD). Statistical analyses were carried out using the two-tailed unpaired *t*-test or Tukey–Kramer multiple comparison tests, if appropriate. $P < 0.05$ was considered significant.

Acknowledgments

The authors express their gratitude to Ms. Sachiko Naito for performing the cell culture and to Mr. Kodai Nishi and Dr. Masato Kobayashi for their helpful discussions.

Masahiro Ono, Shuntaro Oka, Hiroyuki Okudaira, and Yoshifumi Shirakami are employees of Nihon Medi-Physics Co., Ltd. Mark M. Goodman and Emory University have patent rights for *anti*-[^{18}F]FACBC and are eligible to receive royalties on *anti*-[^{18}F]FACBC from Nihon Medi-Physics Co., Ltd. David M. Schuster, Mark M. Goodman, and Keiichi Kawai have ongoing research collaboration with Nihon Medi-Physics Co., Ltd.

REFERENCES

Akhurst, T., Beattie, B., Gogiberidze, G., Montiel, J., Cai, S., Lassman, A., Schoder, H., Pillarsetty, N., Goodman, M., Blasberg, R., 2006. [^{18}F]FACBC Imaging of recurrent gliomas: a comparison with [^{11}C]methionine and MRI. J. Nucl. Med. 47 (suppl. 1), 79.

Bode, B.P., Fuchs, B.C., Hurley, B.P., Conroy, J.L., Suetterlin, J.E., Tanabe, K.K., Rhoads, D.B., Abcouwer, S.F., Souba, W.W., 2002. Molecular and functional analysis of glutamine uptake in human hepatoma and liver-derived cells. Am. J. Physiol. Gastrointest. Liver Physiol. 283, 1062–1073.

Bröer, A., Brookes, N., Ganapathy, V., Dimmer, K.S., Wagner, C.A., Lang, F., Bröer, S., 1999. The astroglial ASCT2 amino acid transporter as a mediator of glutamine efflux. J. Neurochem. 73, 2184–2194.

Bröer, S., Brookes, N., 2001. Transfer of glutamine between astrocytes and neurons. J. Neurochem. 77, 705–719.

Bröer, S., 2006. The SLC6 orphans are forming a family of amino acid transporters. Neurochem. Int. 48, 559–567.

Cho, K.H., Kim, J.Y., Lee, S.H., Yoo, H., Shin, S.H., Moon, S.H., Kim, T.H., Shin, K.H., Yoon, M., Lee, D.H., Pyo, H.R., 2010. Simultaneous integrated boost intensity-modulated radiotherapy in patients with high-grade gliomas. Int. J. Radiat. Oncol. Biol. Phys. 78, 390–397.

Clarke, J., Butowski, N., Chang, S., 2010. Recent advances in therapy for glioblastoma. Arch. Neurol. 67, 279–283.

Fei, Y.J., Sugawara, M., Nakanishi, T., Huang, W., Wang, H., Prasad, P.D., Leibach, F.H., Ganapathy, V., 2000. Primary structure, genomic organization, and functional and electrogenic characteristics of human system N 1, a Na^+- and H^+-coupled glutamine transporter. J. Biol. Chem. 275, 23707–23717.

Fuchs, B.C., Bode, B.P., 2005. Amino acid transporters ASCT2 and LAT1 in cancer: partners in crime? Semin. Cancer Biol. 15, 254–266.

Gegelashvili, M., Rodriguez-Kern, A., Pirozhkova, I., Zhang, J., Sung, L., Gegelashvili, G., 2006. High-affinity glutamate transporter GLAST/EAAT1 regulates cell surface expression of glutamine/neutral amino acid transporter ASCT2 in human fetal astrocytes. Neurochem. Int. 48, 611–615.

Gorlia, T., van den Bent, M.J., Hegi, M.E., Mirimanoff, R.O., Weller, M., Cairncross, J.G., Eisenhauer, E., Belanger, K., Brandes, A.A., Allgeier, A., Lacombe, D., Stupp, R., 2008. Nomograms for predicting survival of patients with newly diagnosed glioblastoma: prognostic factor analysis of EORTC and NCIC trial 26981-22981/CE.3. Lancet Oncol. 9, 29–38.

Herholz, K., Hölzer, T., Bauer, B., Schröder, R., Voges, J., Ernestus, R.I., Mendoza, G., Weber-Luxenburger, G., Löttgen, J., Thiel, A., Wienhard, K., Heiss, W.D., 1998. ^{11}C-methionine PET for differential diagnosis of low-grade gliomas. Neurology 50, 1316–1322.

Kadowaki, M., Yoshioka, H., Kamitani, H., Watanabe, T., Wade, P.A., Eling, T.E., 2012. DNA methylation-mediated silencing of nonsteroidal anti-inflammatory drug-activated gene (NAG-1/GDF15) in glioma cell lines. Int. J. Cancer 15, 267–277.

Kanai, Y., Segawa, H., Miyamoto, K., Uchino, H., Takeda, E., Endou, H., 1998. Expression cloning and characterization of a transporter for a large neutral amino acid activated by the heavy chain of 4F2 antigen (CD98). J. Biol. Chem. 273, 23629–23632.

Kanai, Y., Fukasawa, Y., Cha, S.H., Segawa, H., Chairoungdua, A., Kim, D.K., Matsuo, H., Kim, J.Y., Miyamoto, K., Takeda, E., Endou, H., 2000. Transport properties of a system y^+L neutral and basic amino acid transporter. Insights into the mechanisms of substrate recognition. J. Biol. Chem. 7, 20787–20793.

Kracht, L.W., Miletic, H., Busch, S., Jacobs, A.H., Voges, J., Hoevels, M., Klein, J.C., Herholz, K., Heiss, W.D., 2004. Delineation of brain tumor extent with [^{11}C]L-methionine positron emission tomography: local comparison with stereotactic histopathology. Clin. Cancer Res. 10, 7163–7170.

Laterra, J., Keep, R., Betz, L.A., Goldstein, G.W., 1999. Blood–brain barrier. In: Siegel, G.J., Agranoff, B.W., Albers, R.W., et al. (Eds.), Basic Neurochemistry: Molecular, Cellular and Medical Aspects, 6th ed. Lippincott-Raven, Philadelphia, Available from: ⟨http://www.ncbi.nlm.nih.gov/books/NBK28180/⟩ (last accessed 08.08. 13).

Le Mercier, M., Fortin, S., Mathieu, V., Roland, I., Spiegl-Kreinecker, S., Haibe-Kains, B., Bontempi, G., Decaestecker, C., Berger, W., Lefranc, F., Kiss, R., 2009. Galectin 1 proangiogenic and promigratory effects in the Hs683 oligodendroglioma model are partly mediated through the control of BEX2 expression. Neoplasia 11, 485–496.

Mackenzie, B., Erickson, J.D., 2004. Sodium-coupled neutral amino acid (System N/A) transporters of the SLC38 gene family. Pflugers Arch. 447, 784–795.

Nakanishi, T., Sugawara, M., Huang, W., Martindale, R.G., Leibach, F.H., Ganapathy, M.E., Prasad, P.D., Ganapathy, V., 2001a. Structure, function, and tissue expression pattern of human SN2, a subtype of the amino acid transport system N. Biochem. Biophys. Res. Commun. 281, 1343–1348.

Nakanishi, T., Kekuda, R., Fei, Y.J., Hatanaka, T., Sugawara, M., Martindale, R.G., Leibach, F.H., Prasad, P.D., Ganapathy, V., 2001b. Cloning and functional characterization of a new subtype of the amino acid transport system. N. Am. J. Physiol. Cell Physiol 281, C1757–1768.

Nazzaro, J.M., Neuwelt, E.A., 1990. The role of surgery in the management of supratentorial intermediate and high-grade astrocytomas in adults. J. Neurosurg. 73, 331–344.

Oka, S., Okudaira, H., Yoshida, Y., Schuster, D.M., Goodman, M.M., Shirakami, Y., 2012. Transport mechanisms of trans-1-amino-3-fluoro[1-^{14}C]cyclobutanecarboxylic acid in prostate cancer cells. Nucl. Med. Biol. 39, 109–119.

Okamoto, Y., Sakata, M., Ogura, K., Yamamoto, T., Yamaguchi, M., Tasaka, K., Kurachi, H., Tsurudome, M., Murata, Y., 2002. Expression and regulation of 4F2hc and hLAT1 in human trophoblasts. Am. J. Physiol. Cell Physiol 282, 196–204.

O'Kane, R.L., Viña, J.R., Simpson, I., Hawkins, R.A., 2004. Na^+-dependent neutral amino acid transporters A, ASC, and N of the blood-brain barrier: mechanisms for neutral amino acid removal. Am. J. Physiol. Endocrinol. Metab. 287, 622–629.

Okudaira, H., Shikano, N., Nishii, R., Miyagi, T., Yoshimoto, M., Kobayashi, M., Ohe, K., Nakanishi, T., Tamai, I., Namiki, M., Kawai, K., 2011. Putative transport mechanism and intracellular fate of trans-1-amino-3-^{18}F-fluorocyclobutanecarboxylic acid in human prostate cancer. J. Nucl. Med. 52, 822–829.

Okudaira, H., Nakanishi, T., Oka, S., Kobayashi, M., Tamagami, H., Schuster, D.M., Goodman, M.M., Shirakami, Y., Tamai, I., Kawai, K., 2013. Kinetic analyses of *trans*-1-amino-3-[(18)F] fluorocyclobutanecarboxylic acid transport in *Xenopus laevis oocytes* expressing human ASCT2 and SNAT2. Nucl. Med. Biol. 40, 670–675.

Shao, Z., Kamboj, A., Anderson, C.M., 2009. Functional and immunocytochemical characterization of D-serine transporters in cortical neuron and astrocyte cultures. J. Neurosci. Res. 87, 2520–2530.

Shoup, T.M., Olson, J., Hoffman, J.M., Votaw, J., Eshima, D., Eshima, L., Camp, V.M., Stabin, M., Votaw, D., Goodman, M.M., 1999. Synthesis and evaluation of [^{18}F]1-amino-3-fluorocyclobutane-1-carboxylic acid to image brain tumors. J. Nucl. Med. 40, 331–338.

Sidoryk, M., Matyja, E., Dybel, A., Zielinska, M., Bogucki, J., Jaskólski, D.J., Liberski, P.P., Kowalczyk, P., Albrecht, J., 2004.

Increased expression of a glutamine transporter SNAT3 is a marker of malignant gliomas. Neuroreport 15, 575–578.
SLC tables. Available from: ⟨http://slc.bioparadigms.org/⟩, (last accessed 08.08. 13).
Swanson, K.R., Alvord Jr., E.C., Murray, J.D., 2002. Virtual brain tumours (gliomas) enhance the reality of medical imaging and highlight inadequacies of current therapy. Br. J. Cancer 86, 14–18.
Yu, W., Williams, L., Camp, V.M., Malveaux, E., Olson, J.J., Goodman, M.M., 2009. Stereoselective synthesis and biological evaluation of syn-1-amino-3-[^{18}F]fluorocyclobutyl-1-carboxylic acid as a potential positron emission tomography brain tumor imaging agent. Bioorg. Med. Chem. 17, 1982–1990.
Zhang, X., Lin, Y., Gillies, R.J., 2010. Tumor pH and its measurement. J. Nucl. Med. 51, 1167–1170.